

# *Maximization of Sensitivity to Time-series Polarimetric SAR Image*

Author: *Motofumi Arie*\*

\*Information Technology R&D Center

## Abstract

Understanding the earth's day-to-day changes is an urgent issue for humanity as part of efforts to address global climate change and support recovery from disasters. Synthetic Aperture Radar (SAR) is a technology Mitsubishi Electric has been developing for many years. SAR enables observation day or night, regardless of weather, and is outstanding for detecting, through periodic observation, changes in the earth's surface as differences. Furthermore, Polarimetric SAR (PolSAR) images utilizing the polarization of the SAR transmitting/receiving antennas enable estimation of aspects such as the structure and materials of the observation targets. Mitsubishi Electric has developed a technology for boosting sensitivity to changes in the state of the target, based on PolSAR images observed in a time series, and achieving quantitative measurement without missing even slight differences. We have shown it is possible to quantitatively measure seasonal changes in broad-leaved forests in Hokkaido by applying this technique to PolSAR images taken with the second Advanced Land Observation Satellite (ALOS-2).

## 1. Introduction

When observing earth from space, day-to-day relative changes obtained from time-series images utilizing orbit recurrence are more important than absolute changes obtained from single observations. Unlike an optical camera, SAR is capable of observation day or night, regardless of weather, and if there is no change in the observation target on the earth, there is a high probability that the same power can be received (reproducibility). In addition, sensitivity to the form and material of the observation target is improved by switching polarization characteristics while transmitting and receiving. The PolSAR installed in satellites is particularly outstanding at capturing subtle changes in the earth's surface. Mitsubishi Electric has been involved in the development of all previous satellites equipped with PolSAR functionality by the Japan Aerospace Exploration Agency (JAXA) (Fig. 1). The greatest advantage of PolSAR observation is that once observation is done with two orthogonal polarizations, it is possible to reproduce, offline, the received power corresponding to any transmission/reception polarization. Our company looked again at this basic characteristic of PolSAR images, and developed a technology for quantitatively measuring tiny changes in the observation target with an unprecedented sensitivity.



ALOS-1



ALOS-2



ALOS-4

Fig. 1 PolSAR satellites

## 2. Received Power of PolSAR

Polarization, a fundamental property of electromagnetic waves, is the regular behavior of electric and magnetic fields in a plane perpendicular to the direction of propagation. Such electromagnetic waves are called polarizations and generally have an elliptical shape (Fig.2). In Fig. 2, the propagation direction is perpendicular to the paper surface.

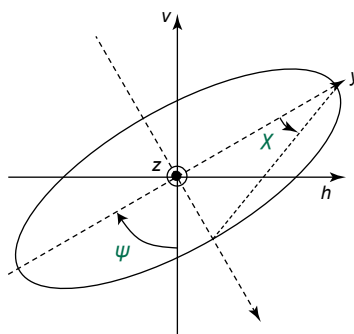


**Fig. 2 Orientation angle  $\psi$  and ellipticity angle  $\chi$  of an electromagnetic wave**

The polarization state  $\vec{p}$  can be expressed as follows using as variables the orientation angle  $\psi$  and the ellipticity angle  $\chi$  that characterize the ellipse.

$$\vec{p}^i = \begin{pmatrix} \hat{p}_h^i \\ \hat{p}_v^i \end{pmatrix} = \begin{bmatrix} \cos \psi^i & \sin \psi^i \\ -\sin \psi^i & \cos \psi^i \end{bmatrix} \begin{bmatrix} j \sin \chi^i \\ \cos \chi^i \end{bmatrix} \quad i = t, r \quad \dots \quad (1)$$

Where,  $t$  and  $r$  stand for transmission and reception, and polarization states can be specified, respectively, for the transmission antenna and reception antenna that constitute the radar equipment (Fig. 3). “ $v_1, v_2, \dots$ ” in Fig. 3 indicate physical quantities of the observation target (such as soil moisture or the plant growth situation).

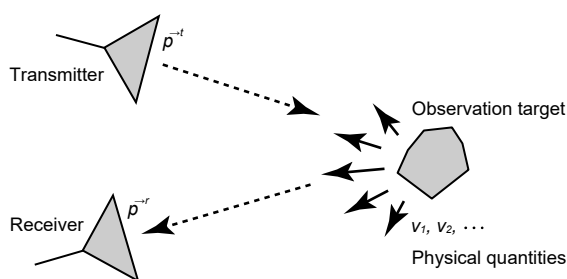


**Fig. 3 PolSAR observation**

That is, the polarization state used for observation can be specified with four variables ( $\psi^t, \chi^t, \psi^r,$  and  $\chi^r$ ). Horizontal polarization and vertical polarization (Fig. 4) are widely used in actual PolSAR observation, and observation is performed while successively switching the polarization state during transmission and reception.

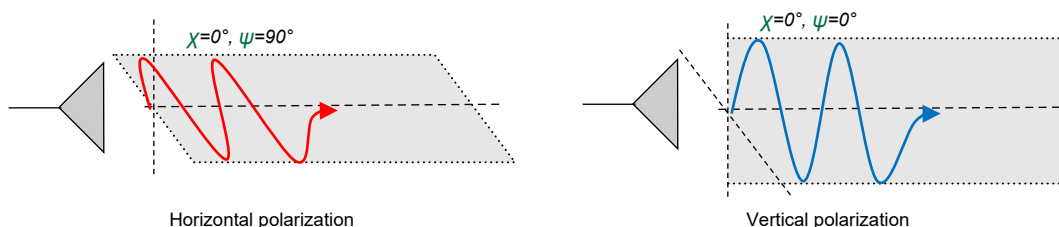


**Fig. 4 Orthogonalized polarization waves**

For example, signals obtained by transmitting vertical polarizations and receiving the scattering from the observation target as horizontal polarizations are called HV polarizations. Through PolSAR observations, HH, HV, VH, and VV polarizations (hereinafter referred to as “standard polarizations”) are recorded. Previous SAR only recorded one of these polarizations. The received power  $P$  can be described using a four-dimensional antenna vector  $\vec{A}$  consisting of  $(\psi^t, \chi^t, \psi^r, \chi^r)$  representing the transmission and receipt polarization states and a 4x4 covariance matrix  $C$  consisting of the radio scattering information from the observation target, as follows:

$$P = \vec{A}(\vec{p}^t(\psi^t, \chi^t), \vec{p}^r(\psi^r, \chi^r))^T C(v_1, v_2, \dots) \vec{A}(\vec{p}^t(\psi^t, \chi^t), \vec{p}^r(\psi^r, \chi^r))^* \dots \dots \dots (2)$$

The scalar  $P$  can be regarded as the brightness of each pixel of the PolSAR image. The covariance matrix constructed through observation can be visualized by the polarization signature<sup>(1)</sup>. Here, visualization was done (Fig. 5) by successively calculating  $P$  while varying  $\psi^t$  and  $\chi^t$ , for the case where the polarization state is the same for transmission and reception (Co-Pol) ( $\vec{p}^t = \vec{p}^r$ ), and the case where they are orthogonal (Cr-Pol) ( $\vec{p}^t \cdot \vec{p}^r = 0$ ).

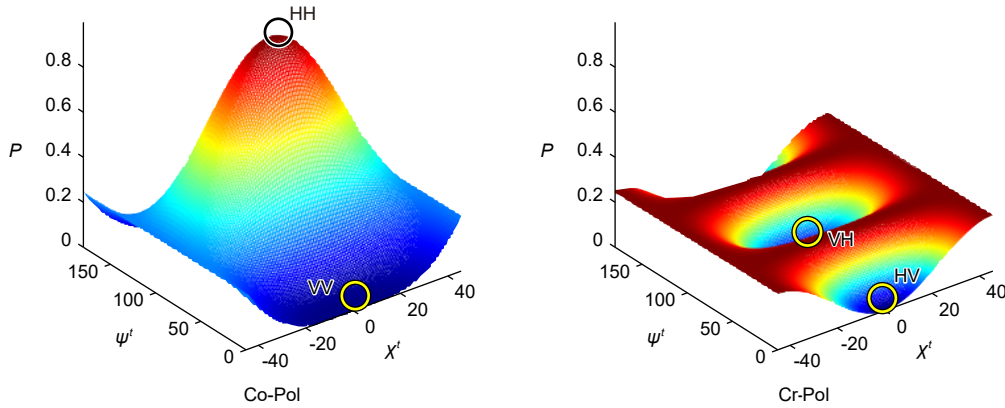


**Fig. 5 Polarization signature of 90° oriented dipole**

The standard polarizations are the powers corresponding to the four points in Fig. 5. In previous SAR, only one of these points was observed. However, the covariance matrix obtained with PolSAR contains a great deal of information besides that. This means that once a covariance matrix is constructed with two orthogonal polarizations, it is possible in principle to reproduce the power of any transmission-reception polarization state. This property is the one of the most important features of PolSAR. For example, it has been used as a technique for emphasizing contrast of two observation targets (e.g., ships vs. the ocean surface) in the same image<sup>(2)</sup>. In this paper, the property is applied to high-sensitivity detection of quantitative change in time-series PolSAR images. In Fig. 5, the maximum power just happens to be captured by the HH polarization ( $\chi^t=0^\circ, \psi^t=90^\circ$ ) but that depends on the condition of the observation target and is not always the case.

**3. Technique for Maximizing Sensitivity to Differences**

The discussion in this section 3 is based on PolSAR images of two scenes with different observation times. The power difference due to the change in state of the observation target during this period can be described as follows.

$$\Delta P = P(t_1) - P(t_0) = \vec{A}(\psi^t, \chi^t, \psi^r, \chi^r)^T \{C(t_1) - C(t_0)\} \vec{A}(\psi^t, \chi^t, \psi^r, \chi^r)^* \dots \dots \dots (3)$$

This shows that the power difference can be maximized, in the following way, by appropriately selecting  $\vec{A}$ , provided there is a change in the observation target.

$$(\psi_{opt}^t, \chi_{opt}^t, \psi_{opt}^r, \chi_{opt}^r) = \max_{\psi^t, \chi^t, \psi^r, \chi^r} \left| \frac{\partial P(\psi^t, \chi^t, \psi^r, \chi^r, \dots)}{\partial t} \right| \dots \dots \dots (4)$$

The optimal polarization state can be found by applying the method of Lagrange multiplier.

To illustrate the specific processing method based on this principle, the following example shows a case where the same region was observed four times during the period from  $t_0$  to  $t_3$  (Fig. 6).

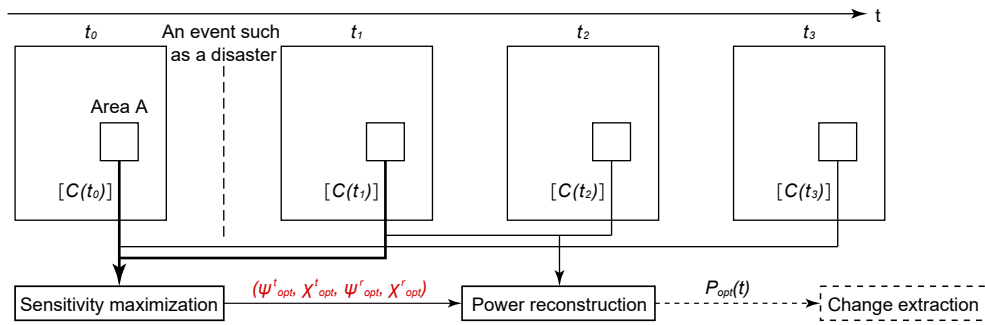


**Fig. 6 Algorithm of a maximization of polarimetric sensitivity**

It is assumed that, in the interval between  $t_0$  and  $t_1$ , a major change occurs due to an event such as a disaster, and after that there is a gradual recovery at  $t_2$  and  $t_3$ . First, the optimal angles that maximize the difference  $(\psi^{t_{opt}}, \chi^{t_{opt}}, \psi^{r_{opt}}, \chi^{r_{opt}})$  are found from the PolSAR images for  $t_0$  and  $t_1$ , where change is the greatest, and these are stored for each pixel. Next, the power at each time is reconstructed by applying the stored optimal angles to Equation<sup>(2)</sup> in section 2. By using the same antenna vector  $\vec{A}$   $(\psi^{t_{opt}}, \chi^{t_{opt}}, \psi^{r_{opt}}, \chi^{r_{opt}})$  in all periods in this way, it is possible to establish a standard for comparing change, and the change in the target can be localized to  $|C(t_1)-C(t_0)|$ . The differences between arbitrary images from the four reconstructed PolSAR images enable quantitative analysis as changes in the state of the target. On the other hand, the optimal angle itself can be a new physical parameter representing the state of the observation target.

**4. Validation: Maximizing Sensitivity to Forest Growth**

ALOS-2 was used to observe the broad-leaved forest in Tomakomai City in Hokkaido at three times ( $t_0$ : December 30, 2018;  $t_1$ : January 27, 2019; and  $t_2$ : August 11, 2019). The technique examined in section 3 was applied to those PolSAR images. As is evident in the photos in Fig. 7, there are conspicuous time series changes characteristic of deciduous trees.



**Fig. 7 Snapshots taken in deciduous forest of Tomakomai**

Figure 8 shows HH polarization images of the same region. From  $t_0$  to  $t_1$ , there is only the difference of one month in the winter season, just a small change, But from  $t_1$  to  $t_2$ , there is a marked increase in brightness due to leaf growth from winter to summer.

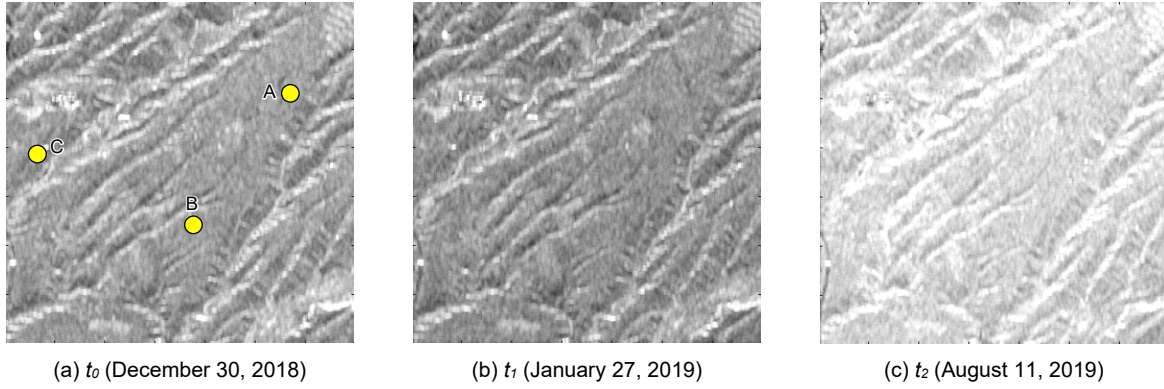


Fig. 8 Time-series PolSAR images obtained by ALOS-2 (HH)

Here, sensitivity is maximized for  $t_0$  and  $t_2$ , where the maximum change is expected. For locations A to C indicated in Fig. 8(a), the results of power reconstruction after sensitivity maximization are shown in Fig. 9. To emphasize sensitivity, Fig. 8(b) and (c) are shown as the power difference at an arbitrary time and  $t_0$ .

At all locations, received power shows an increasing trend in accordance with growth. Valid results are obtained, with the reconstructed power ( $P_{OPT}$ ) becoming maximal at  $t_2$ , and exhibiting natural changes including  $t_1$ . This technique enables quantitative analysis of physical changes in the target region, based on differences of arbitrary pairs, because the standard for comparison during the period is the same.

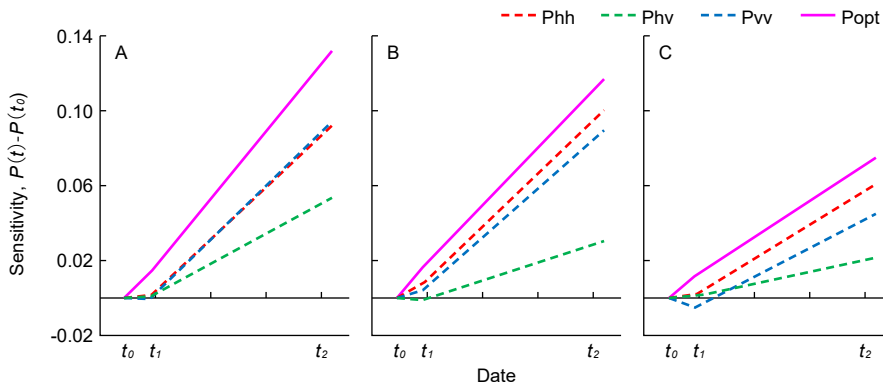


Fig. 9 Time histories of the received power and its sensitivity in areas A-C of Fig. 8(a)

To validate this technique for the entire image, Fig. 10 shows the difference images of  $t_0$  and  $t_2$  after power reconstruction.

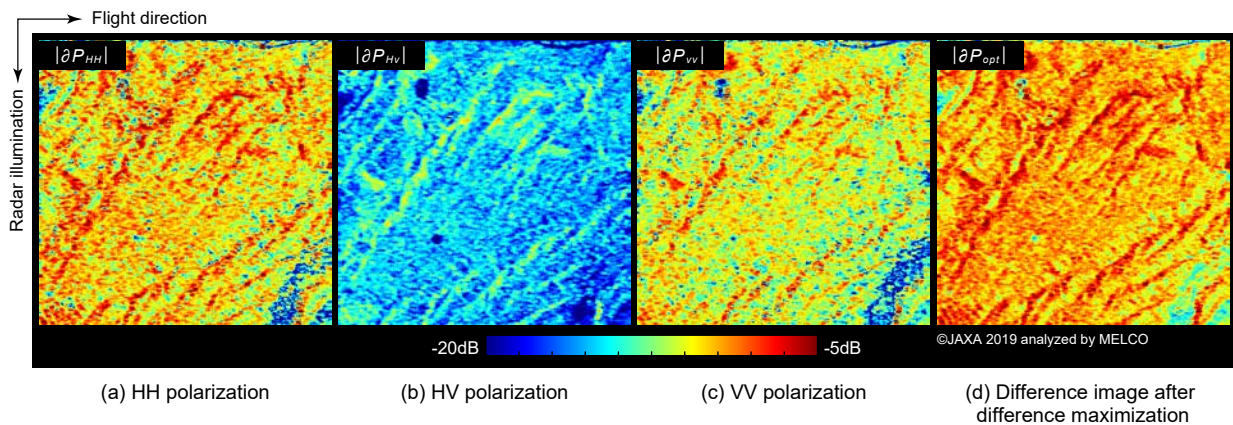
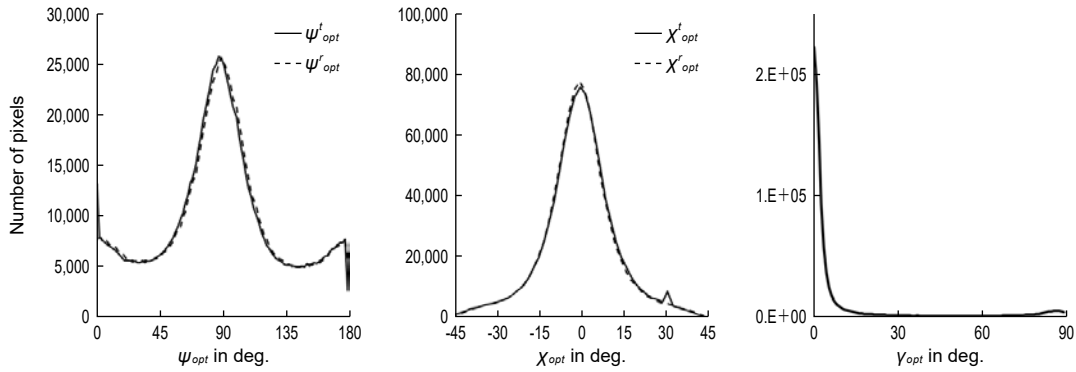


Fig. 10 Comparison of optimized difference map (right) with those of standard polarizations between  $t_0$  and  $t_2$

The HH image (Fig. 10(a)) is the difference of Fig. 8(a)  $t_0$  and (c)  $t_2$ . It is evident that, over the entire range of the image, the magnitude of the change due to the proposed technique (Fig. 10(d)) is maximal. Also, the angle formed by the transmission-reception polarization state is defined as follows, taking the obtained optimal angle as a new physical quantity.

$$\cos\gamma_{opt} = \frac{\vec{P}_{opt}^t \cdot \vec{P}_{opt}^r}{|\vec{P}_{opt}^t| |\vec{P}_{opt}^r|} \dots\dots\dots (5)$$

Histograms of  $\psi_{opt}$ ,  $\chi_{opt}$ , and  $\gamma_{opt}$  in the image range of the ALOS-2 image (Fig. 8) are shown in Fig. 11.



**Fig. 11 Histograms of optimized polarimetric angles  $\psi_{opt}$  (left),  $\chi_{opt}$  (center), and  $\gamma_{opt}$  (right) of ALOS-2 image of Fig. 8**

$\psi_{opt}$  and  $\chi_{opt}$  exhibit almost equal distributions in transmission and reception, and respectively have mean values near  $90^\circ$  (horizontal polarization) and  $0^\circ$  (linear polarization). For  $\gamma_{opt}$ , it was shown quantitatively that almost all pixels indicate  $0^\circ$  (transmission and reception polarization state are equal), and for the pertinent region as a whole, sensitivity is high near HH polarization ( $90^\circ$ ), but there is also a considerable distribution at other orientation angles.

**5. Conclusion**

This paper describes a technique used with PolSAR images to maximize time series sensitivity and quantitatively measure changes in arbitrary observation targets. The proposed technique was applied to PolSAR images observed in time series with ALOS-2, and it was confirmed that differences can be maximized. It was also shown that more various information for each observation target can be extracted by using the optimal polarization state itself that is obtained for each pixel. Mitsubishi Electric will apply this technology to the monitoring of forest growth for global warming countermeasures and the extraction of disaster areas caused by flooding due to linear precipitation zones, which have been rapidly increasing in recent years. By combining this technology with the PolSAR satellite development technology we have cultivated over the years, Mitsubishi Electric will continue to provide technology that enables quantitative and precise understanding of global changes in the earth’s surface on a global scale.

**References**

- (1) Jakob, J. van Zyl: On the Importance of Polarization in Radar Scattering Problems, Ph. D. Thesis, California Institute of Technology (1985)
- (2) Swartz, A. A., et al.: The Optimal Polarizations for Achieving Maximum Contrast in Radar Images, Journal of Geophysical Research, 93, No.B12, 15252–15260 (1988)